American Mineralogist, Volume 67, pages 1179–1194, 1982

Ferri-annite from the Dales Gorge Member iron-formations, Wittenoom area, Western Australia

TAKASHI MIYANO[1]

Department of Geology
Indiana University
Bloomington, Indiana 47405

AND SUMIKO MIYANO

Institute of Geoscience
The University of Tsukuba
Ibaraki 305, Japan

Abstract

Ferri-annite, a new, naturally occurring mica with a representative composition of $K_{1.82}(Mg_{1.83}Fe^{2+}_{4.23})(Fe^{3+}_{1.69}Al_{0.28}Si_{6.02})O_{20}(OH)_4$, probably expressed by the quadrilateral components annite, phlogopite, ferri-annite ($K_2Fe^{2+}_6Fe^{3+}_2Si_6O_{20}(OH)_4$), and ferri-phlogopite ($K_2Mg_6Fe^{3+}_2Si_6O_{20}(OH)_4$), is described from the Wittenoom area, Western Australia. The mineral occurs as flaky to tabular grains or as massive aggregates of fine acicular grains near or within a riebeckite-rich zone of banded iron-formation, the Dales Gorge Member of the Hamersley Group. It coexists with hematite, magnetite, quartz, ankerite, stilpnomelane, and riebeckite. The ferri-annite can be chemically subdivided into two groups, A and B. The group A variety contains 4 to 7 wt.% Al_2O_3 and has light reddish brown (=*X*) to pale yellow green (=*Y,Z*) pleochroism, and the B variety, with the lowest Al_2O_3 content (1 to 2 wt.%), has brownish red (=*X*) to pale greenish brown (=*Y,Z*) pleochroic colors. The latter variety generally contains about 10 wt.% more Fe than the former. (001) cleavage is perfect. Twinning is frequent. Cell parameters (*a, b, c,* β, *V*) of the mica (group B) were calculated as 5.402(6), 9.237(4), 10.306(7)Å, 99°16′(10), and 507.54(67)Å^3 using X-ray powder diffraction analysis. Formation of much of the ferri-annite appears to be the result of potassium enrichment in stilpnomelane concomittant with the formation of associated riebeckite.

Introduction

Veres *et al.* (1955) and Wones (1963a) have described the synthetic iron mica (ferri-annite), $K_2Fe^{2+}_3(Fe^{3+}Si_3)O_{10}(OH)_2$, and the phase equilibria of ferri-annite have been examined by Wones (1963a). The crystal structure of this mica was determined to be a trioctahedral one-layer mica (1M) by Donnay *et al.* (1964). The mica synthesized by Wones (1963a) was formed at conditions of oxygen fugacity between those of the HM and WI buffers, at 400–850°C, and at 1035 and 2070 bars ($=P_{H_2O} + P_{H_2}$). He suggested that mica with a composition such as ferri-annite might be found in iron-formations resulting from magmatic conditions. However, such a mica has not been found in iron-formations of magmatic origin. Foster (1960) showed that biotites containing tetrahedral ferric iron are frequently found in alkaline rocks and pegmatites. Such biotites, however, contain 6 to 15 wt.% more Al_2O_3 than the ferri-annite of this study.

Naturally Fe-rich and Al-poor mica (hereafter referred to as ferri-annite) occurs in the very low-grade iron-formation of the Dales Gorge Member, Hamersley Group, Western Australia. Mineral assemblages involving ferri-annite (Fe-rich mica) have been described and their petrologic significance has been discussed by Miyano (1982).

The purpose of this paper is to describe the mineralogy, chemical composition, and cell parameters of the ferri-annite.

[1]Permanent address: Institute of Geoscience, The University of Tsukuba, Ibaraki 305, Japan.

0003–004X/82/1112–1179$02.00

Occurrence, paragenesis, and optical properties

Flaky to tabular mica grains with a diameter of 10 to 40 μm are dispersed in chert-rich mesobands that are close to or within a riebeckite-rich band or zone (Fig. 1A). They coexist with quartz, hematite, magnetite, stilpnomelane, riebeckite, and ankerite, and are oriented nearly parallel to the sedimentary structure. Massive aggregates of fine-grained ferri-annite commonly form thin, lenticular and discontinuous bands up to about 0.2 mm thick, alternating with iron-oxide microbands (Fig. 1B). Stilpnomelane is commonly replaced by ferri-annite where they coexist (Fig. 1C). Textures suggest that the bands now occupied by ferri-annite may originally have been stilpnomelane bands. In some occurrences, however, the mica is found as veinlets in chert (Fig. 1D); such veinlets originate in stilpnomelane bands.

The mica appears to be later in formation than the other silicates except riebeckite. Textural relations between ferri-annite and riebeckite are complex. Both minerals occur in a similar manner around or along magnetite grains or bands (Fig. 1E, F), where the mica is flaky and coarser than the needle-like (fibrous) riebeckite. It may be that Al released from stilpnomelane during replacement by riebeckite has been reprecipitated as ferri-annite close to riebeckite bands (Miyano, 1982). However, prismatic grains of riebeckite commonly cut across both ferri-annite and fibrous riebeckite bands. Fibrous riebeckite (also crocidolite) is much more abundant than prismatic riebeckite. If there were two stages of formation for riebeckite, the mica may well be contemporaneous with the first stage of fibrous riebeckite formation.

Ferri-annite occurs in two colored varieties under the microscope, one with light reddish brown ($=X$) to pale yellow green ($=Y,Z$) pleochroism, and the other with brownish red ($=X$) to pale greenish brown ($=Y,Z$) pleochroic colors, which are very similar to those of synthetic ferri-annite of Wones (1963a, p. 583). The latter variety is generally fine-grained and constitutes massive aggregates which may resemble ferristilpnomelane. The former (with light reddish brown to pale yellow green color) often occurs as flaky to tabular grains or aggregates. In the flaky grains, (001) cleavage is perfect but not as well-developed as in biotite. Twinning is frequent. Because of the limited amount of material, only approximate refractive indices could be obtained. There are:

light reddish brown ($=X$)

$$\alpha = 1.653 \pm 0.005$$
$$\gamma = 1.691 \pm 0.005$$
$$\gamma\text{-}\alpha = 0.038 \sim 0.044$$
$$2V_x = 0° \sim 10°$$

brownish red ($=X$)

$$\alpha = 1.677 \pm 0.005$$
$$\gamma = 1.721 \pm 0.005$$
$$\gamma\text{-}\alpha = 0.045 \sim 0.052$$
$$2V_x = \text{small}$$

Chemical composition

The chemical composition of the ferri-annite was obtained by electron microprobe, and is shown in Tables 1, 2, and 3. Table 1 shows chemical compositions of flaky to tabular grains of ferri-annite (Sample Z, anal. 1 to 3; DE, anal. 4 to 6; GE, anal. 7 to 9) and fibrous to acicular grains which form massive aggregates (Sample MA, anal. 10 to 12), in various assemblages. Table 2 represents chemical analyses of fibrous to acicular grains, forming massive aggregates, of mica with the lowest Al_2O_3 contents (Sample MB). Both mica types (samples MA and MB) commonly form lenticular and discontinuous bands, but the MB type is more coarsely crystallized and makes thicker bands than type MA. Table 3 represents average chemical compositions of the mica in both occurrences.

The composition of the mica can be described by K_2O, MgO, FeO, Fe_2O_3, Al_2O_3, and SiO_2 (other components are minor and total less than one percent) and can be chemically subdivided into two groups, A and B. Group A contains 4 to 7 wt.% Al_2O_3 and 28 to 33 wt.% FeO (total Fe), and group B 1 to 2 wt.% Al_2O_3 and 38 to 43 wt.% FeO (total Fe) (Tables 1 to 3). The former shows light reddish brown to pale yellow green pleochroism and the latter brownish red to pale greenish brown pleochroic colors. The chemical differences between ferri-annite and other micas such as biotite and phlogopite, are depicted in Figures 2 and 3, with total iron of all micas recalculated as FeO. The ferri-annites contain much less Al_2O_3 than biotite and phlogopite. The ideal compositions of micas on the join annite ($K_2Fe^{2+}_6Al_2Si_6O_{20}(OH)_4$)–ferri-annite ($K_2Fe^{2+}_6Fe^{3+}_2Si_6O_{20}(OH)_4$) show that the K_2O content of ferri-annite is usually less than that of the ideal formula (Fig. 2). Associated stilpnomelane, an Fe-rich phyllosilicate can also be divided into two

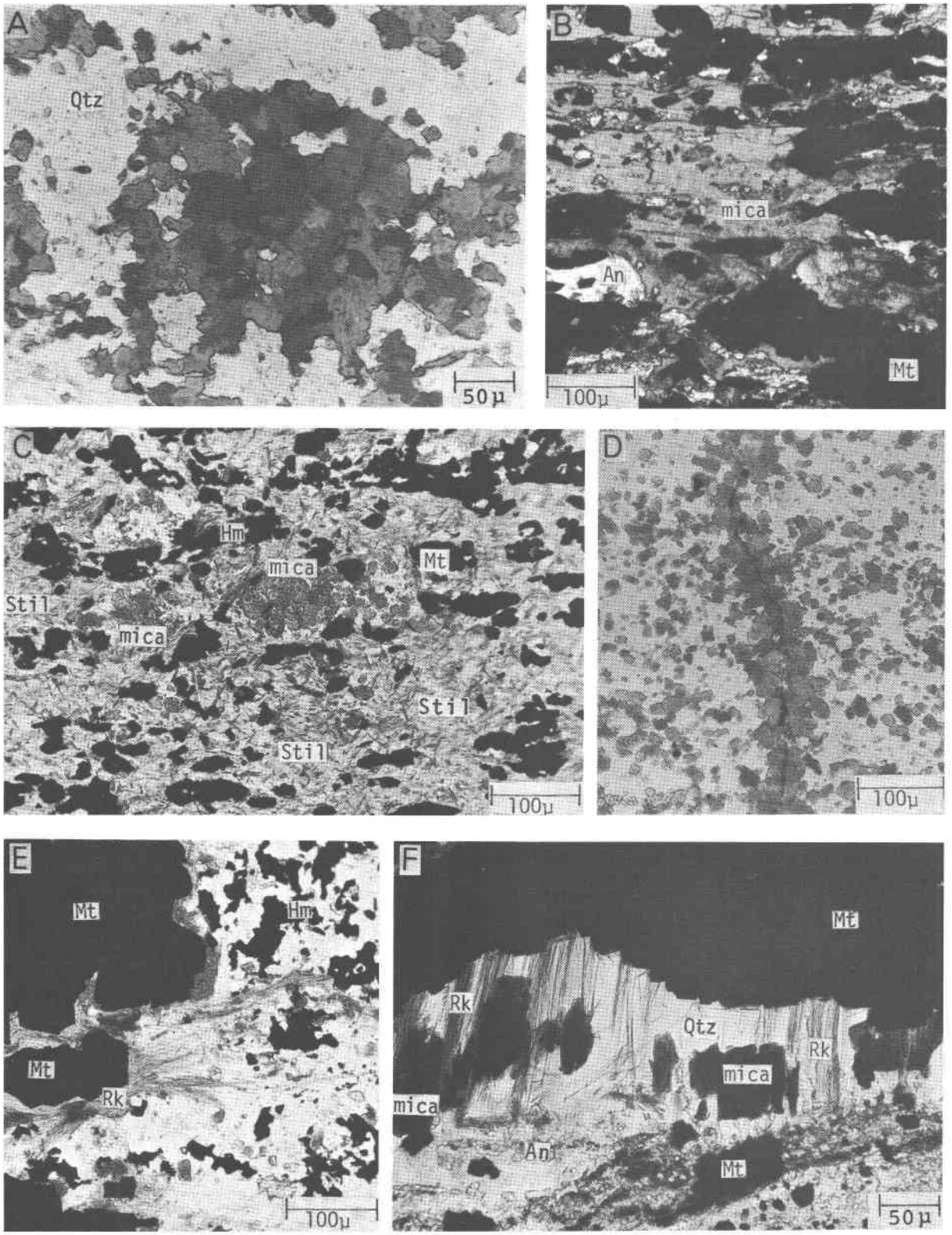

Fig. 1. Some occurrences of ferri-annite. (A) Aggregates of flaky to tabular grains of ferri-annite in a chert-rich band. Grey to dark colored portions with high index, showing twinning, are ferri-annite. Sample GE. Polarized light. (B) Massive aggregates of fine, acicular grains of ferri-annite (mica, grey). Black parts are hematite and magnetite. Sample MB. Polarized light. (C) Ferri-annite (mica) in a massive stilpnomelane band. Black portions are hematite and magnetite. This stilpnomelane is enriched in potassium. Sample GE. Polarized light. (D) Veinlet of ferri-annite in chert. Black euhedral grains are magnetite. Flaky grains are disseminated along the veinlet. Sample GE. Polarized light. (E) Needlelike riebeckite and flaky ferri-annite (grey) around euhedral magnetite grains (black) in a chert-rich band. Black irregular grains are hematite. Sample DE. Polarized light. (F) Needlelike (fibrous) riebeckite and flaky to tabular ferri-annite (mica) are intergrown with quartz along a magnetite band. Small black dots in the lower right corner are hematite. Sample Z. Polarized light.

Table 1. Representative electron microprobe analyses of ferri-annite from the Dales Gorge Member iron-formations

Wt. %	1 Z115	2 Z131	3 Z278	4 DE3	5 DE18	6 DE20	7 GE328	8 GE340	9 GE352	10 MA368	11 MA373	12 MA379
SiO_2	38.01	39.02	35.79	39.33	38.93	39.69	38.56	39.13	37.71	36.49	35.76	36.20
Al_2O_3	6.19	5.58	5.31	5.37	4.71	5.04	5.40	5.86	6.37	1.89	1.79	1.92
TiO_2	0.05	0.00	0.00	0.04	0.00	0.00	0.00	0.02	0.00	0.00	0.01	0.00
Cr_2O_3	0.01	0.00	0.01	--	--	--	--	--	--	--	--	--
FeO*	29.68	29.11	33.80	28.95	30.52	29.79	30.43	31.33	30.34	40.29	40.80	39.80
MnO	0.02	0.00	0.01	0.02	0.09	0.03	0.00	0.05	0.00	0.00	0.01	0.03
NiO	0.07	0.04	0.00	--	--	--	--	--	--	--	--	--
MgO	12.03	12.50	11.70	12.72	12.17	12.55	11.70	10.81	12.48	7.37	7.50	7.85
CaO	0.04	0.00	0.01	0.03	0.02	0.00	0.01	0.01	0.01	0.01	0.02	0.01
Na_2O	0.06	0.09	0.00	0.04	0.04	0.02	0.09	0.00	0.36	0.08	0.01	0.04
K_2O	8.21	7.49	8.30	8.53	8.32	8.57	8.38	8.35	8.30	7.80	7.73	7.56
Total	94.37	93.83	94.93	95.03	94.80	95.69	94.57	95.56	95.57	93.93	93.63	93.41
Fe_2O_3**	6.28	6.14	9.67	6.71	7.66	7.05	6.77	5.76	7.07	11.57	12.30	11.76
FeO	24.03	23.59	25.10	22.92	23.62	23.44	24.34	26.15	23.98	29.88	29.73	29.22
Total	95.00	94.45	95.90	95.71	95.56	96.39	95.25	96.14	96.28	95.09	94.86	94.59
					Cations on the basis of 22 oxygens							
Si	6.078	6.216	5.805	6.205	6.198	6.234	6.167	6.215	5.970	6.155	6.070	6.121
Al	1.167	1.048	1.015	0.999	0.884	0.932	1.018	1.097	1.188	0.376	0.358	0.383
Fe^{3+}	0.755	0.736	1.180	0.796	0.918	0.834	0.815	0.688	0.842	1.469	1.572	1.496
Σ	8.000	8.000	8.000	8.000	8.000	8.000	8.000	8.000	8.000	8.000	8.000	8.000
Ti	0.006	0.000	0.000	0.005	0.000	0.000	0.000	0.002	0.000	0.000	0.001	0.000
Cr	0.001	0.000	0.001	--	--	--	--	--	--	--	--	--
Fe^{2+}	3.214	3.143	3.405	3.024	3.146	3.079	3.256	3.474	3.175	4.215	4.221	4.132
Mn	0.003	0.000	0.001	0.003	0.012	0.004	0.000	0.007	0.000	0.000	0.001	0.004
Ni	0.009	0.005	0.000	--	--	--	--	--	--	--	--	--
Mg	2.868	2.969	2.829	2.992	2.889	2.938	2.790	2.560	2.945	1.853	1.898	1.979
Σ	6.101	6.117	6.236	6.024	6.047	6.021	6.046	6.043	6.120	6.068	6.121	6.115
Ca	0.007	0.000	0.002	0.005	0.003	0.000	0.002	0.002	0.002	0.002	0.004	0.002
Na	0.019	0.028	0.000	0.012	0.012	0.006	0.028	0.000	0.110	0.026	0.003	0.013
K	1.675	1.522	1.717	1.717	1.690	1.717	1.710	1.692	1.676	1.679	1.674	1.631
Σ	1.701	1.550	1.719	1.734	1.705	1.723	1.740	1.694	1.788	1.707	1.681	1.646
$Fe^{2+}/Fe^{2+}+Mg$	0.528	0.514	0.546	0.503	0.521	0.512	0.539	0.576	0.519	0.695	0.690	0.676

*All Fe as FeO. **estimated from tetrahedral ferric iron (see text). The ratio $Fe^{2+}/(Fe^{2+}+Mg)$ in the bottom line, the same as in Tables 2 and 3, is calculated after subtraction of tetrahedral ferric iron from total FeO. Samples Z, DE, and GE: flaky to tabular grains (group A), sample MA: massive aggregates of acicular grains (group B). Sample DE was analyzed at the Geological Survey of Japan (G.S.J.), and the others at the Analytical Center of the University of Tsukuba (A.C.U.T.). 1. Mt-Hm-Qt-Mica. 2. Hm-Mt-Mica. 3. Rk-Mica-Stil-Mt-Hm. 4. Rk-Qt-Mica-Mt-Hm±An. 5. Qt-Mica-An-Hm-Mt. 6. Mica-Qt-Mt-Hm±Rk. 7. Mica-Qt-Mt (mica veinlet, Fig. 1D). 8. Qt-Mica-Mt-An. 9. Mica-Qt-Stil-Mt-Hm. 10. Mica-Rk-Hm. 11. Rk-Hm-Mica-Qt±Mt. 12. An-Qt-Mica-Hm±Mt.

Mineral abbreviations (through the text): An=ankerite, Hm=hematite, Ho-hornblende, K-fel=K-feldspar, Mica=ferri-annite, Mt=magnetite, Qt=quartz, Po=pyrrhotite, Py=pyrite, Stil=stilpnomelane.

Table 2. Representative electron microprobe analyses of ferri-annite with the lowest Al_2O_3 content from the Dales Gorge Member

Wt. %	1 MB479	2 MB480	3 MB484	4 MB485	5 MB487	6 MB488	7 MB491	8 MB492
SiO_2	35.81	35.28	35.93	35.97	35.16	35.08	35.41	35.57
Al_2O_3	1.46	1.31	1.36	1.19	1.46	1.33	1.38	1.36
TiO_2	0.00	0.04	0.00	0.03	0.01	0.01	0.03	0.03
Cr_2O_3	0.00	0.03	0.05	0.02	0.00	0.07	0.00	0.00
FeO*	41.45	42.09	41.43	41.65	41.82	42.41	42.03	41.69
MnO	0.00	0.00	0.00	0.03	0.01	0.00	0.07	0.09
NiO	0.03	0.11	0.05	0.00	0.00	0.09	0.08	0.00
MgO	7.25	7.01	7.05	7.38	7.14	7.21	7.21	7.16
CaO	0.06	0.03	0.02	0.04	0.00	0.10	0.06	0.07
Na_2O	0.00	0.01	0.02	0.00	0.00	0.03	0.02	0.04
K_2O	8.11	8.16	8.11	8.12	8.28	7.76	7.87	7.91
Total	94.17	94.07	94.02	94.43	93.88	94.09	94.16	93.92
Fe_2O_3**	12.83	13.40	12.71	13.24	13.23	13.70	13.34	13.08
FeO	29.90	30.03	29.99	29.73	29.91	30.08	30.03	29.92
Total	95.45	95.41	95.29	95.75	95.20	95.46	95.50	95.23
	Cations on the basis of 22 oxygens							
Si	6.071	6.017	6.103	6.079	6.005	5.976	6.018	6.053
Al	0.292	0.263	0.272	0.237	0.294	0.267	0.276	0.273
Fe^{3+}	1.637	1.720	1.625	1.684	1.701	1.757	1.706	1.674
Σ	8.000	8.000	8.000	8.000	8.000	8.000	8.000	8.000
Ti	0.000	0.005	0.000	0.004	0.001	0.001	0.004	0.004
Cr	0.000	0.004	0.007	0.003	0.000	0.009	0.000	0.000
Fe^{2+}	4.240	4.283	4.261	4.203	4.273	4.285	4.268	4.259
Mn	0.000	0.000	0.000	0.004	0.001	0.000	0.010	0.013
Ni	0.004	0.015	0.007	0.000	0.000	0.012	0.011	0.000
Mg	1.832	1.782	1.785	1.859	1.818	1.831	1.827	1.816
Σ	6.076	6.089	6.060	6.073	6.093	6.138	6.120	6.092
Ca	0.011	0.005	0.004	0.007	0.000	0.018	0.011	0.013
Na	0.000	0.003	0.007	0.000	0.000	0.010	0.007	0.013
K	1.754	1.775	1.757	1.751	1.804	1.687	1.706	1.717
Σ	1.765	1.783	1.768	1.758	1.804	1.715	1.724	1.743
$Fe^{2+}/Fe^{2+}+Mg$	0.698	0.706	0.705	0.693	0.702	0.701	0.700	0.701

*All Fe as FeO. **estimated from tetrahedral ferric iron. Analyzed at A.C.U.T. Massive aggregates of ferri-annite, coexisting mainly with magnetite and hematite, and a small amount of quartz, ankerite, and riebeckite (see Fig. 1B).

Table 3. Average electron microprobe analyses of ferri-annite

Wt. %	1 Z (18)	S.D.	2 DE (18)	S.D.	3 GE (24)	S.D.	4 MA (15)	S.D.	5 MB (16)	S.D.	6
SiO_2	38.50	0.77	38.47	0.63	38.44	0.77	36.23	0.31	35.49	0.28	33.33
Al_2O_3	5.43	0.48	5.00	0.59	5.84	0.49	1.83	0.11	1.42	0.15	
TiO_2	0.02	0.02	0.03	0.04	0.02	0.02	0.01	0.01	0.01	0.02	
Cr_2O_3	0.02	0.03	--	--	--	--	--	--	0.02	0.02	
Fe_2O_3*	6.84	0.96	7.70	1.00	6.65	0.52	11.98	0.29	13.25	0.53	14.77
FeO	23.62	0.70	23.26	0.43	25.15	0.89	29.57	0.54	29.77	0.31	39.86
MnO	0.03	0.04	0.04	0.03	0.03	0.04	0.02	0.02	0.03	0.03	
NiO	0.02	0.04	--	--	--	--	--	--	0.04	0.04	
MgO	12.05	0.44	12.45	0.39	11.50	0.66	7.56	0.31	7.24	0.18	
CaO	0.04	0.04	0.03	0.03	0.01	0.02	0.02	0.02	0.05	0.03	
Na_2O	0.06	0.10	0.06	0.04	0.15	0.18	0.06	0.10	0.02	0.02	
K_2O	8.46	0.45	8.28	0.43	8.30	0.13	7.87	0.21	8.33	0.27	8.71
Total	95.09	0.72	95.32	0.56	96.09	0.39	95.15	0.70	95.67	0.72	96.67
	cations on the basis of 22 oxygens										
Si	6.154		6.136		6.111		6.115		6.024		6.000
Al	1.023		0.940		1.094		0.364		0.284		
Fe^{3+}	0.823		0.924		0.795		1.521		1.692		2.000
Σ	8.000		8.000		8.000		8.000		8.000		8.000
Ti	0.002		0.004		0.002		0.001		0.001		
Cr	0.003		--		--		--		0.003		
Fe^{2+}	3.157		3.102		3.344		4.174		4.226		6.000
Mn	0.004		0.005		0.004		0.003		0.004		
Ni	0.003		--		--		--		0.005		
Mg	2.872		2.960		2.725		1.902		1.832		———
Σ	6.041		6.071		6.075		6.080		6.071		6.000
Ca	0.007		0.005		0.002		0.004		0.009		
Na	0.019		0.019		0.046		0.020		0.007		
K	1.725		1.685		1.683		1.695		1.804		2.000
Σ	1.751		1.709		1.731		1.719		1.820		2.000
$Fe^{2+}/Fe^{2+}+Mg$	0.524		0.512		0.551		0.687		0.698		1.000

*estimated from tetrahedral ferric iron. Number in parentheses is the number of analytical points. S.D. standard deviation (1σ). Including chemical compositions listed in Tables 1 and 2. 6: Ideal composition of ferri-annite.

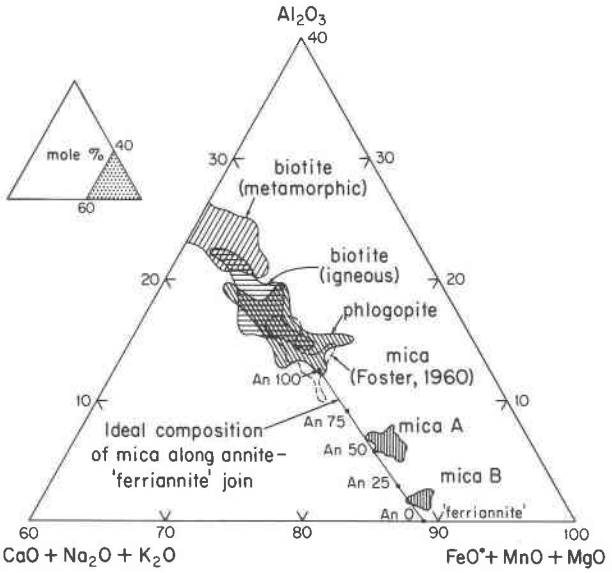

Fig. 2. Graphical representation of chemical analyses of biotite, phlogopite, and ferri-annite. Micas A and B refer to ferri-annites of group A and B, respectively. The data for biotite and phlogopite are taken from Deer *et al.* (1962). The area enclosed by a dashed line represents trioctahedral micas with tetrahedral ferric iron of Foster (1960). FeO* indicates all Fe in micas recalculated as FeO. Solid line with An markings shows the ideal composition along the annite (An 100)–ferri-annite (An 0) join.

groups, A and B, by using the ratio Fe*/(Fe* + Mg) where Fe* indicates total Fe. Such ratios for ferri-annite in groups A and B are nearly the same as those for stilpnomelane in the respective groups as shown in Figure 3. According to Miyano (1982), the Fe/(Fe+Mg) ratio increases with decreasing f_{O_2}, which implies that stilpnomelane in group A may reflect higher f_{O_2} conditions than that in group B. This same ratio in ferri-annite, however, seems to be independent of variations of f_{O_2}, as judged from its occurrence with both hematite and/or magnetite.

The number of ions per formula unit, recalculated on the basis of 22 oxygens and assuming no tetrahedral Fe, shows a cation of deficiency in the tetrahedral sites (less than 8 by 1 to 2 cations) and a cation excess in the octahedral sites (greater than 6 by 1 to 2 cations). This means that the tetrahedral Al-position is in part filled by ferric iron. Such a substitution has been proposed for some natural biotites by Foster (1960). Her micas, with tetrahedral ferric iron, are plotted in Figure 1. Steinfink (1962) determined the crystal structure of a natural iron-rich phlogopite (ferri-phlogopite) with some ferric iron located in the tetrahedral sites. Synthetic ferri-annite with tetraheral iron also has been reported by Veres *et al.* (1955) and Wones (1963a). Fe^{2+} and Fe^{3+} cannot, however, be distinguished by electron microprobe analysis. Assuming that all Fe^{3+}, Al, and Si of the mica are located in tetrahedral sites totalling 8 cations, the minimum amount of Fe_2O_3 can be estimated as shown in Tables 1 to 3. As a result, the number of octahedral cations ranges from 6.0 to 6.2 (close to ideal) and the $Fe^{2+}/(Fe^{2+} + Mg)$ ratios of the micas are a relatively constant value. The number of silicons is usually greater than 6.0 and the number of cations in the interlayer positions commonly less than 2.0. The Si values greater than 6.0 and the sum of the octahedral cations may be related to the general deficiency of cations (K,Na,Ca) in the interlayer positions. This deficiency, however, is unlikely to have much effect on either the ratio of $Fe^{2+}/(Fe^{2+}+Mg)$ in the octahedral sites or on $Fe^{3+}/(Fe^{3+}+Al)$ in the tetrahedral sites.

The compositional variations of the ferri-annites of this study may be expressed by four end-members: annite ($K_2Fe^{2+}_6Al_2Si_6O_{20}(OH)_4$), ferri-annite ($K_2Fe^{2+}_6Fe^{3+}_2Si_6O_{20}(OH)_4$), phlogopite ($K_2Mg_6Al_2Si_6O_{20}(OH)_4$), and ferri-phlogopite ($K_2Mg_6Fe^{3+}_2Si_6O_{20}(OH)_4$), in terms of the ratios of $Fe^{2+}/(Fe^{2+}+Mg)$ and $Fe^{3+}/(Fe^{3+}+Al)$ as shown in Figure 4. The variations are generally limited within relatively narrow ranges of the ratios of $Fe^{2+}/(Fe^{2+} + Mg)$ and $Fe^{3+}/(Fe^{3+}+Al)$. The one exception is the $Fe^{3+}/(Fe^{3+}+Al)$ ratio of mica sample DE, which ranges from about 0.4 to 0.7. As seen in Figure 4,

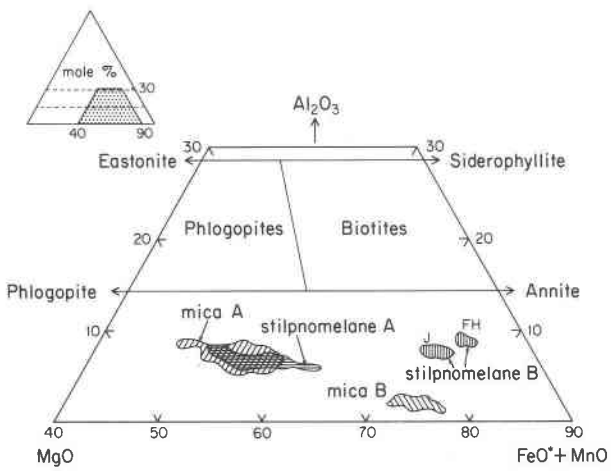

Fig. 3. Graphical representation of chemical compositions of biotite, phlogopite, ferri-annite, and stilpnomelane. FeO* indicates all Fe in micas recalculated as FeO. Groups A and B of ferri-annite and stilpnomelane show the distinctive ratios of Fe/(Fe+Mg).

Table 4. Representative electron microprobe analyses of stilpnomelane (group A) coexisting with ferri-annite and/or riebeckite

Wt. %	1 Z262	2 Z265	3 Z259	4 Z268	5 Z258	6 B447	7 B423	8 B432	9 B424	10 B426
SiO_2	47.61	46.30	47.28	45.82	46.32	49.83	47.87	49.62	49.45	48.79
Al_2O_3	4.19	4.53	4.34	5.06	5.25	4.31	4.51	4.39	4.44	4.25
TiO_2	0.02	0.02	0.00	0.01	0.00	0.00	0.03	0.02	0.00	0.01
Cr_2O_3	0.00	0.01	0.00	0.00	0.00	0.00	0.01	0.00	0.00	0.00
FeO*	26.45	26.92	25.88	25.91	24.60	24.10	25.15	25.45	24.27	24.67
MnO	0.10	0.12	0.09	0.08	0.25	0.00	0.03	0.01	0.00	0.00
NiO	0.00	0.00	0.01	0.00	0.00	0.00	0.01	0.05	0.00	0.00
MgO	9.43	9.85	10.87	10.87	11.05	9.50	9.65	9.64	9.67	9.70
CaO	0.01	0.03	0.02	0.01	0.01	0.04	0.05	0.01	0.03	0.04
Na_2O	0.04	0.00	0.15	0.00	0.11	0.00	0.51	0.13	0.54	1.49
K_2O	1.75	3.15	4.94	5.82	7.03	2.15	2.88	3.81	5.46	7.20
Total	89.60	90.93	93.58	93.58	94.62	89.93	90.70	93.13	93.86	96.15
	cations on the basis of 22 oxygens									
Si	7.477	7.276	7.249	7.086	7.087	7.666	7.437	7.513	7.477	7.338
Al	0.523	0.724	0.751	0.914	0.913	0.334	0.563	0.487	0.523	0.662
Σ	8.000	8.000	8.000	8.000	8.000	8.000	8.000	8.000	8.000	8.000
Al	0.253	0.115	0.033	0.008	0.034	0.447	0.263	0.296	0.268	0.091
Ti	0.002	0.002	0.000	0.000	0.000	0.000	0.004	0.002	0.000	0.001
Cr	0.000	0.001	0.000	0.000	0.000	0.000	0.001	0.000	0.000	0.000
Fe^{2+}	3.474	3.538	3.319	3.351	3.148	3.101	3.268	3.223	3.069	3.103
Mn	0.013	0.016	0.012	0.010	0.032	0.000	0.004	0.001	0.000	0.000
Ni	0.000	0.000	0.001	0.000	0.000	0.000	0.001	0.006	0.000	0.000
Mg	2.208	2.308	2.485	2.506	2.521	2.179	2.235	2.176	2.180	2.175
ΣA	5.950	5.980	5.850	5.875	5.735	5.727	5.776	5.704	5.517	5.370
Ca	0.002	0.005	0.003	0.002	0.002	0.007	0.008	0.002	0.005	0.006
Na	0.012	0.000	0.045	0.000	0.033	0.000	0.154	0.038	0.158	0.434
K	0.351	0.632	0.966	1.148	1.372	0.422	0.571	0.736	1.053	1.381
ΣB	0.365	0.637	1.014	1.150	1.407	0.429	0.733	0.776	1.216	1.821
ΣA+ΣB	6.315	6.617	6.864	7.025	7.142	6.156	6.509	6.480	6.733	7.191
Fe*/Fe*+Mg	0.611	0.605	0.572	0.572	0.555	0.587	0.594	0.597	0.585	0.588

*All Fe as FeO. Analyzed at A.C.U.T. Sample Z (1 to 5): Stil(brown)-Mica-Mt-Rk(+Ho)-Qt. It is possible that some compositions are a mixture of stilpnomelane and ferri-annite (see text). Sample B (6 to 10): Stil(pale green)-Hm-Qt-An-Rk-Mt. Note variable K_2O contents. 1: From Miyano (1982).

Table 5. Representative electron microprobe analyses of stilpnomelane (group B) coexisting with neither ferri-annite nor riebeckite

Wt. %	1 J288	2 J299	3 J295	4 J286	5 J298	6 FH3	7 FH4	8 FH5
SiO_2	45.02	45.42	45.36	44.91	44.75	46.08	45.76	46.34
Al_2O_3	4.02	4.59	4.77	4.65	4.91	5.16	5.17	5.71
TiO_2	0.00	0.00	0.00	0.00	0.00	0.00	0.01	0.08
FeO*	33.52	32.54	32.33	32.97	32.29	32.82	32.42	32.19
MnO	0.21	0.05	0.04	0.06	0.03	0.00	0.13	0.10
MgO	4.49	4.73	5.01	4.75	5.03	3.76	4.00	3.89
CaO	0.23	0.09	0.02	0.01	0.04	0.03	0.02	0.07
Na_2O	0.24	0.42	0.48	2.03	1.43	0.23	0.23	0.19
K_2O	2.32	3.02	3.66	4.64	5.13	1.44	1.39	1.49
Total	90.05	90.86	91.67	94.02	93.61	89.52	89.13	90.06
	cations on the basis of 22 oxygens							
Si	7.391	7.364	7.310	7.176	7.165	7.481	7.458	7.446
Al	0.609	0.636	0.690	0.824	0.835	0.519	0.542	0.554
Σ	8.000	8.000	8.000	8.000	8.000	8.000	8.000	8.000
Al	0.169	0.241	0.216	0.052	0.091	0.468	0.451	0.527
Ti	0.000	0.000	0.000	0.000	0.000	0.000	0.001	0.010
Fe^{2+}	4.602	4.412	4.357	4.406	4.324	4.456	4.419	4.326
Mn	0.029	0.007	0.005	0.008	0.004	0.000	0.018	0.014
Mg	1.099	1.143	1.204	1.131	1.201	0.910	0.972	0.932
ΣA	5.899	5.803	5.782	5.597	5.620	5.834	5.861	5.809
Ca	0.040	0.016	0.003	0.002	0.007	0.005	0.003	0.012
Na	0.076	0.132	0.150	0.629	0.444	0.072	0.073	0.059
K	0.486	0.625	0.752	0.946	1.048	0.298	0.289	0.305
ΣB	0.602	0.773	0.905	1.577	1.499	0.375	0.365	0.376
ΣA+ΣB	6.501	6.576	6.687	7.714	7.119	6.209	6.226	6.185
Fe*/Fe*+Mg	0.807	0.794	0.784	0.796	0.783	0.830	0.820	0.823

*All Fe as FeO. Sample J (1 to 5) was analyzed at A.C.U.T. and sample FH (6 to 8) at G.S.J. Sample J: Stil-An-Mt-Py. Sample FH: Stil-An-K-Fel-Py-Po.

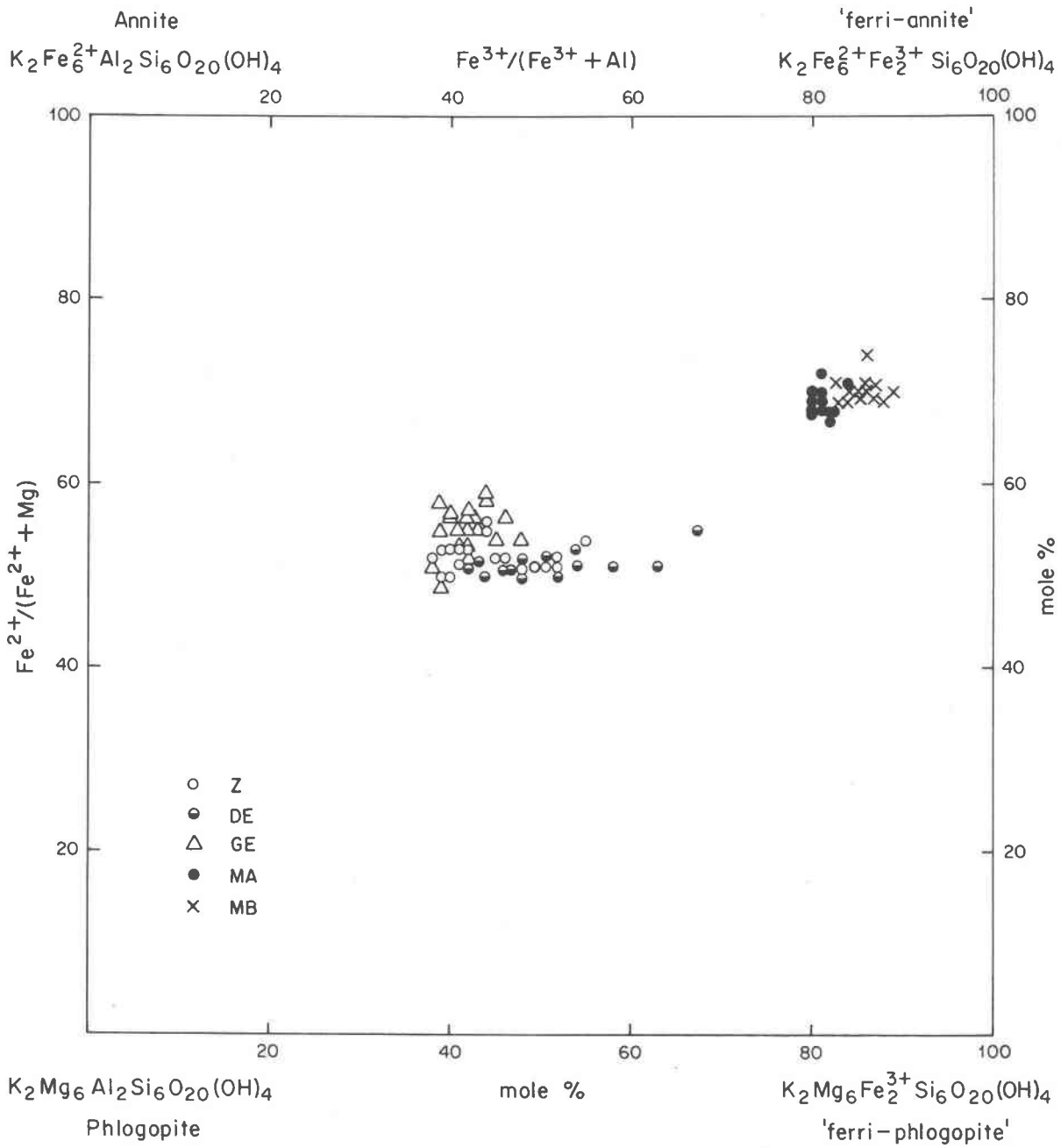

Fig. 4. Quadrilateral representation of ferri-annite.

one may identify one group of the ferri-annites as annite and the other as ferri-annite, because the $Fe^{2+}/(Fe^{2+}+Mg)$ ratios of both groups are greater than 0.5.

After having subtracted the calculated ferric iron content from total FeO, the ferri-annite compositions may be depicted in terms of cations in the interlayer ($CaO + Na_2O + K_2O$), octahedral ((FeO) + MnO + MgO), and tetrahedral (Al_2O_3) positions, as shown in Figure 5 (A, B). If any iron is present in the octahedral sites, it is treated as ferrous. Figure 5 shows a more realistic representation of the chemical composition of the ferri-annites than does Figure 2 and also plots not only all ferri-annites but stilpnomelane as well.

X-ray crystallography

Because of fine grain size of the massive aggregates and the limited amount of material, neither

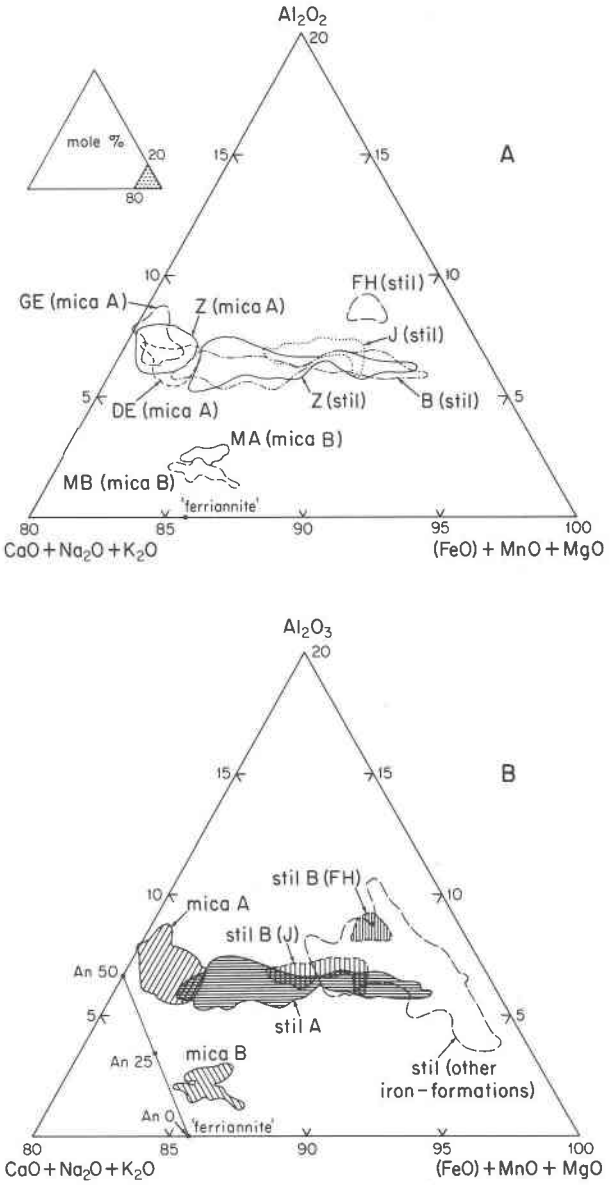

Fig. 5. Graphical representation of chemical variations of ferri-annite and stilpnomelane. (FeO) means that FeO for mica does not include ferric iron estimated from the tetrahedral site occupancy, but all Fe in stilpnomelane is expressed as FeO. Figure A shows the variations of the two minerals in several occurrences of the Dales Gorge Member. Figure B depicts the variation of stilpnomelane in other iron formations (dashed lines) for comparison. Note the wide variation of K_2O content of stilpnomelane.

single crystals nor concentrates of ferri-annite could be separated for X-ray investigation. Accordingly, a band relatively rich in ferri-annite within banded iron-formation was used for this purpose. Such a layer usually contains small amounts of impurities such as hematite, magnetite, quartz, ankerite, and riebeckite. Magnetite was removed by a hand magnet. Three samples, GE, MA, and MB, taken from this type of layer, were carefully separated under the microscope. Samples GE and MB include very small amounts of magnetite, ankerite, and riebeckite. A small amount of ankerite is present in sample MA. However, hematite and quartz could not be completely removed from samples MA and MB because small grains of both minerals are present within the layers.

The samples were analyzed by X-ray powder techniques (Fe$K\alpha$). Using silicon (a = 5.4307Å) as an internal standard, five to eight d-spacings were measured on a diffractometer. The X-ray powder data are given in Table 6, and were indexed with a monoclinic setting. The following unit-cell parameters were determined on sample MB: a = 5.402(6), b = 9.237(4), c = 10.306(7)Å, β = 99°16′(10), and 507.54(67)Å^3, by means of a least squares method (program UNICS RSLC-3) using all reflections except $\bar{1}13$) listed in Table 6. These parameters are comparable with those of annite (Eugster and Wones, 1962), ferri-phlogopite (Steinfink, 1962), and ferri-annite (Morimoto and Donnay, 1961; Wones, 1963a) (see Table 7). Table 7 shows, however, that the b dimension of the ferri-annite is remarkably smaller than that of other Fe-rich micas. The parameters of b and β are rather similar to those of

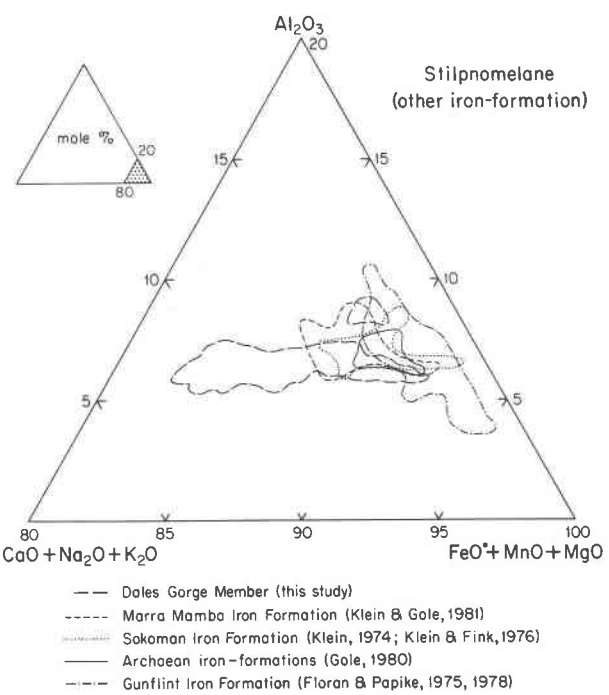

Fig. 6. Graphical comparison of chemical variations of stilpnomelane from various iron-formations.

Table 6. X-ray powder data for ferri-annite (Fe$K\alpha$)

	GE		MA		MB		Ferri-annite (1)		Ferri-annite' (2)		
hkl	d(Å)	I*	d(Å)	I*	d(Å)	I*	d(Å)	I**	d(Å)	I***	I(INT)
001	10.139	VS	10.163	M	10.159	VS	10.180	100	10.163	100	100
$\bar{1}12$	3.686	VW	3.683	W	3.684	M	3.736	5	3.721	7	9
003	3.379	M			3.379	M	3.394	65	3.388	17	25
$\bar{1}13$			2.903	VW	2.905	VW	2.950	6	2.959	5	8
200	2.646	VW			2.666	VW	2.673	45	2.674	24	13
133			2.044	W					2.028	4	6
$\bar{2}04$			2.039						2.026		3
006					1.696	M	1.699	10	1.694	4	1
242					1.600	W			1.611	1	1
060	1.539	W	1.539	W	1.539	VW	1.567	20	1.567	6	5

GE, MA, and MB: this study (Mn filter; Slit 1°, 0.3, 1°; scan speed 0.25 o/min; chart speed; 20mm/min; T.C. 2; scale 800 cps).
(1): Wones (1963), powder data.
(2): Morimoto and Donnay (1961), Donnay et al. (1964), Borg and Smith (1969) single crystal-data.
I*: relative intensity: VS=very strong, S=strong, M=medium; W=weak, VW=very weak.
I**: I/Io on arbitrary scale.
I***: peak intensity from the simulated diffractometer trace.
I(INT): relative integrated intensity normalized to a maximum value of 100.

Table 7. Cell parameters and refractive indices of ferri-annite and related micas

	1	2	3	4	5
	annite	ferri-phlogopite	ferri-annite	ferri-annite	ferri-annite
a(Å)	5.391 (±0.01)	5.36 (±0.01)	5.43 (±0.01)	5.430 (±0.002)	5.402 (±0.006)
b(Å)	9.348 (±0.004)	9.29 (±0.02)	9.40 (±0.01)	9.404 (±0.003)	9.237 (±0.004)
c(Å)	10.313 (±0.02)	10.41 (±0.02)	10.33 (±0.01)	10.341 (±0.006)	10.306 (±0.007)
β	99°42' (±15')	100°0' (±10')	100°10' (±15')	100°4' (±10')	99°16' (±10')
α	1.625 (±0.002)	-	1.705 (±0.005)		1.677 (±0.005)
γ	1.691 (±0.002)	-	1.748 (±0.003)		1.721 (±0.005)

1. Eugster and Wones (1962), $AnFe_6$, powder data.
2. Steinfink (1962), $(K_{0.9}Mn_{0.1})Mg_3(FeSi_3)O_{10}(OH)_2$, single-crystal data.
3. Morimoto and Donnay (1961), $KFe_3(FeSi_3)O_{10}(OH)_2$, single-crystal data.
4. Wones (1963), $KFe_3(FeSi_3)O_{10}(OH)_2$, powder data.
5. This study, sample MB, powder data.

biotite (a = 5.30, b = 9.21, c = 10.16Å, and β = 99°18′; Donnay and Ondik, 1973).

According to Wones (1963b), the b dimension of synthetic biotite on the phlogopite-annite join decreases with decreasing Fe/(Fe+Mg) ratio, and with increasing oxygen fugacity. Synthetic ferri-annite used for the determination of cell parameters was formed in the stability field of wüstite and fayalite (probably between the MW and WI buffers; Wones, 1963a; Donnay *et al.*, 1964). Because ferri-annite usually coexists with hematite and magnetite and commonly contains MgO (Fe*/(Fe* + Mg) = 0.75–0.78, group B), the b dimension may be shortened more than that of pure ferri-annite. On the other hand, Donnay *et al.* (1964) show in their structural model that the length of the K–O bond of ferri-annite restricts the length of b more severely than either d_t (tetrahedral metal–oxygen distance) of d_o (octahedral metal–anion distance), and that the K–O distance of the mica is surprisingly large (=3.05Å). If we assume that the same values for d_t and d_o as those of Donnay *et al.* (1964) for the ferri-annite, our b dimension (=9.237Å) gives the normal K–O bond length of 2.83Å.

Origin of ferri-annite

Because of the intimate association of ferri-annite and stilpnomelane, the chemical composition of the mica may well be related to that of the stilpnomelane. Especially, the similarity of the ratio of Fe*/(Fe* + Mg) between the two minerals is remarkable as already mentioned.

In one sample (Z) a ferri-annite layer grades transitionally into a stilpnomelane layer, and thin fibrous riebeckite and magnetite bands (0.2 to 0.3 mm thick) are present between the two layers. Magnetite occurs in both layers but hematite only in the mica layer. The stilpnomelane layer consists mainly of aggregates of interlocking laths of stilpnomelane and partly of Fe-rich mica as judged from the X-ray powder diffraction pattern (Fig. 7). However, the chemical analyses of the laths do not show the typical composition of either stilpnomelane or ferri-annite because they contain a higher K_2O content than "normal" stilpnomelane whereas the other oxide contents are similar to those of stilpnomelane (Table 4, sample Z, anal. 2 to 5). Because of the presence of X-ray reflections for mica, it appears that the composition may be equivalent to a mixture of stilpnomelane and ferri-annite. As shown in Table 4, the K_2O content ranges from 1.8 to 7.0 wt.%. Such a range in K_2O content is also

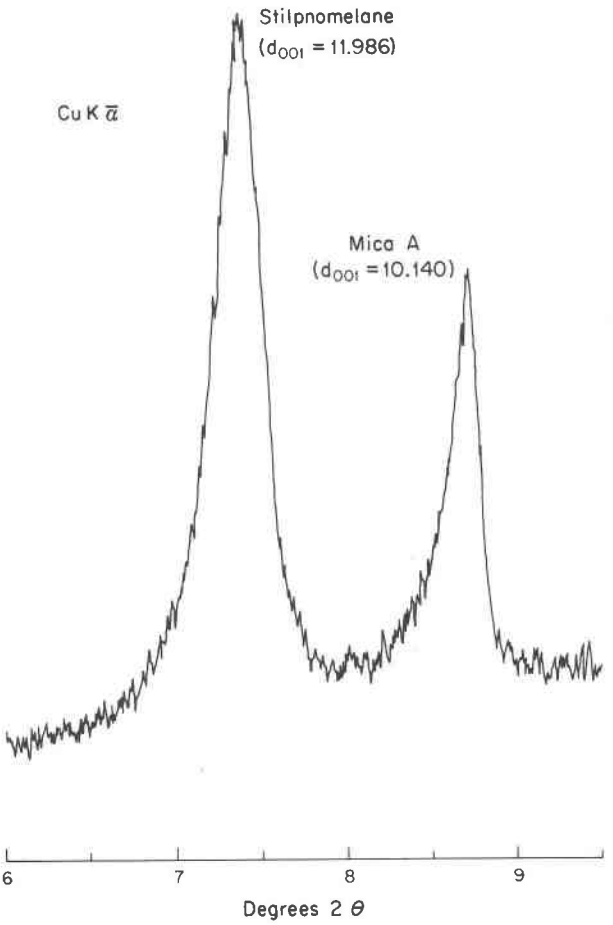

Fig. 7. X-ray reflections (d_{001} in Å) of stilpnomelane and ferri-annite (Cu$K\alpha$).

found in stilpnomelanes close to a fibrous riebeckite band (Table 1, sample B), where the X-ray powder diffraction pattern shows no extra peak for mica. Generally, stilpnomelanes with high K_2O contents (>3 wt.%) have commonly been reported from iron-formations with a large amount of riebeckite (LaBerge, 1966a,b; Trendall and Blockley, 1970; Ayres, 1972; Klein and Gole, 1981; Miyano, 1982; also see Tables 4 and 5). The variation of the K_2O content of stilpnomelane in the Dales Gorge Member is shown in Figure 5A. Comparison with those of other iron-formations is made in Figures 5B and 6. These figures show that stilpnomelane of the Dales Gorge Member is more alkali-rich than that of other iron-formations. A similar tendency is found in riebeckite-containing assemblages in the Marra Mamba Iron Formation (Klein and Gole, 1981). Miyano (1982) proposed that ferri-annite (and also some riebeckite) may replace stilpnomelane as a

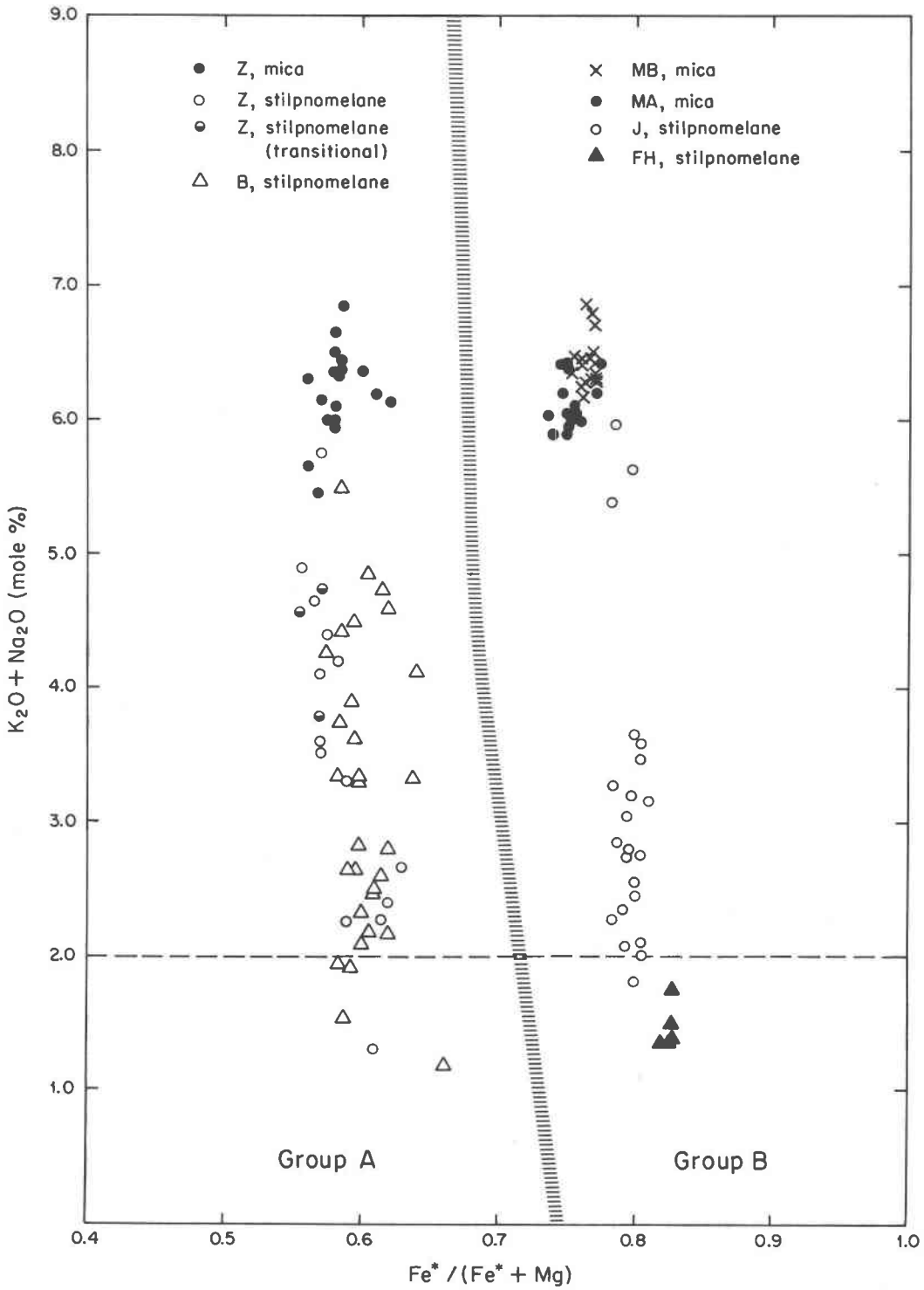

Fig. 8. Compositions of stilpnomelane and ferri-annite in terms of $K_2O + Na_2O$ content (mol%) and Fe*/(Fe* + Mg) ratio. The area below the dashed line shows the K_2O content of "normal" stilpnomelane. In sample Z, the K_2O content (group A) increases continuously from that of "normal" stilpnomelane to that of ferri-annite.

result of interaction with alkali-bearing solutions, which may also have been responsible for the formation of riebeckite. This interaction appears to accompany enrichment of alkalies in stilpnomelane prior to replacement by ferri-annite. However, some parts of the Dales Gorge Member rocks seem not to have been affected by such alkali-bearing solutions, because the K_2O content of stilpnomelane in such rocks is "normal" as shown in Table 5 (sample FH, anal. 6 to 8). Using chemical analyses listed in Tables 1, 2, 4, and 5 and preliminary analytical data on stilpnomelane and ferri-annite, this feature can be illustrated as a function of (K_2O + Na_2O) mole percent against the variation of Fe*/(Fe* + Mg) as in Figure 8. In the case of sample Z (group A), the $K_2O(+Na_2O)$ content of stilpnomelane increases continuously toward that of ferri-annite at a constant ratio of Fe*/(Fe* + Mg). Figure 8 also shows mica and stilpnomelane in other occurrences, including those in group B. No stilpnomelane with a high ratio of Fe*/(Fe* + Mg) was found to be associated with ferri–annite in this study. However, sample J contains stilpnomelane of group B and it has a wide variation of K_2O content as shown in Table 5, probably as a result of action of alkali-bearing solutions. The X-ray powder diffraction pattern of this stilpnomelane shows only stilpnomelane peaks. This stilpnomelane may be regarded as a precursor of the ferri-annite of group B (samples MA and MB), because the variation in K_2O content from stilpnomelane to mica is similar to that demonstrated for sample Z (Figure 8). It is of interest that the stilpnomelane of samples B (group A) and J (group B) which contain little ferri-annite, shows a relatively higher Na_2O content than stilpnomelane that coexist with ferri-annite. It appears that much of the ferri-annite may have formed from stilpnomelane by secondary enrichment of potassium at a fixed Fe*/(Fe*+Mg) ratio, and that Fe^{2+} may have been oxidized to Fe^{3+} in order to fill the cation deficiency in the tetrahedral sites. It is probable that such potassium enrichment and oxidation may have been brought about by alkali-bearing solutions, but the presence of "normal" stilpnomelane shows that such enrichment has not been uniform throughout the entire member.

Conclusions

Ferri-annite, from a very low-grade metamorphic iron-formation, the Dales Gorge Member of Western Australia, is defined on the basis of mineralogical, chemical, and X-ray powder data. Much of this mica may have formed from stilpnomelane by enrichment of potassium during metamorphism. Because of cation deficiency in the tetrahedral sites if tetral Fe is excluded, the mica composition may be expressed by quadrilateral components: annite, phlogopite, ferri-annite ($K_2Fe^{2+}_6Fe^{3+}_2Si_6O_{20}(OH)_4$) and ferri-phlogopite ($K_2Mg_6Fe^{3+}_2Si_6O_{20}(OH)_4$). Cell parameters of the mica are, however, somewhat different from those predicted from the quadrilateral components. The differences may be due to the conditions of formation of the mica. Further refinement and characterization of this mica must wait until pure, crystalline material is available in sufficient amounts.

Acknowledgments

This work was begun while one of the authors (T.M.) was a post-doctoral fellow in 1976 of the Association of Japanese Academic Promotion at Tokyo University of Education. Part of this study was supported by a Grant-in-Aid for Encouragement of Young Scientists (574326) of the Ministry of Education, Science and Culture of Japan. Further funding was provided by NSF grant EAR 80-20377 to C. Klein. Electron microprobes were used at the Analytical Center of Tsukuba University and at the Geological Survey of Japan. T. M. is grateful to A. Sasaki and K. Okumura at the Geological Survey of Japan and to N. Nishida of Tsukuba University for their help in obtaining microprobe data. We thank Y. Suzuki, S. Sueno, and M. Kimata for obtaining X-ray powder data; Messrs. W. H. Moran, R. T. Hill, and G. R. Ringer for drafting and photography of the illustrations; Mrs. Thea Brown for the typing of the manuscript; and C. Klein and A. Kato for their critical and constructive reviews which considerably improved its content.

References

Ayres, D. E. (1972) Genesis of iron-bearing minerals in banded iron formation mesobands in the Dales Gorge Member, Hamersley Group, Western Australia. Economic Geology, 67, 1214–1233.

Borg, I. Y. and Smith, D. K. (1969) Calculated X-ray powder patterns for silicate minerals. Geological Society of America, Memoir 122.

Donnay, G., Morimoto, N., Takeda, H., Donnay, J. D. H. (1964) Trioctahedral one-layer micas. Acta Crystallographica, 17, 1369–1381.

Donnay, J. D. H. and Ondik, H. M. (1973) Crystal Data. Determinative tables 3rd ed., Vol. 2, Inorganic Compounds. U. S. Department of Commerce, National Bureau of Standards (NSRDS).

Eugster, H. P. and Wones, D. R. (1962) Stability relations of the ferruginous biotite, annite. Journal of Petrology, 3, 82–125.

Foster, M. D. (1960) Interpretation of the composition of trioctahedral micas. U. S. Geological Survey Professional Paper 354-B, 11–49.

Klein, C. and Gole, M. J. (1981) Mineralogy and petrology of parts of the Marra Mamba Iron-Formation, Hamersley Basin, Western Australia. American Mineralogist, 66, 507–525.

LaBerge, G. L. (1966a) Altered pyroclastic rocks in South African iron-formation. Economic Geology, 61, 572–581.

LaBerge, G. L. (1966b) Altered pyroclastic rocks in iron-formation in the Hamersley Range, Western Australia. Economic Geology, 61, 147–161.

Miyano, T. (1982) Stilpnomelane, Fe-rich mica, K–feldspar, and hornblende in banded iron-formation assemblages of the Dales Gorge Member, Hamersley Group, Western Australia. Canadian Mineralogist, 20, 189–202.

Morimoto, N. and Donnay, J. D. H. (1961) Crystal structure of synthetic iron mica. Carnegie Institution of Washington Year Book 1960–1961, 214–215.

Steinfink, H. (1962) Crystal structure of a trioctahedral mica. American Mineralogist, 47, 886–896.

Trendall, A. F. and Blockley, J. G. (1970) The iron formations of the Precambrian Hamersley Group, Western Australia. Geological Survey of Western Australia, Bulletin 119.

Veres, G. I., Merenkova, T. B., and Ostrovskii, I. A. (1955) Synthetic pure iron hydroxyl mica (in Russian). Akademie Nauk SSSR Doklady, 101, 147–150.

Wones, D. R. (1963a) Phase equilibria of "ferriannite", $KFe_3^{+2}Fe^{+3}Si_3O_{10}(OH)_2$. American Journal of Science, 261, 581–596.

Wones, D. R. (1963b) Physical properties of synthetic biotites on the join phlogopite–annite. American Mineralogist, 48, 1300–1321.

Manuscript received, October 12, 1981;
accepted for publication, June 18, 1982.